

Topological change of the Fermi surface in ternary iron-pnictides with reduced c/a ratio: A dHvA study of CaFe_2P_2

Amalia I. Coldea,¹ C.M.J. Andrew,¹ J.G. Analytis,^{2,3} R.D. McDonald,⁴
A.F. Bangura,¹ J.-H. Chu,^{2,3} I.R. Fisher,^{2,3} and A. Carrington¹

¹*H.H. Wills Physics Laboratory, University of Bristol, Tyndall Avenue, Bristol, BS8 1TL, UK*

²*Stanford Institute for Materials and Energy Sciences,*

SLAC National Accelerator Laboratory, 2575 Sand Hill Road, Menlo Park, CA 94025, USA

³*Geballe Laboratory for Advanced Materials and Department of Applied Physics, Stanford University, USA*

⁴*Los Alamos National Laboratory, Los Alamos, NM 87545, USA*

(Dated: May 20, 2009)

We report a de Haas-van Alphen effect study of the Fermi surface of CaFe_2P_2 using low temperature torque magnetometry up to 45 T. This system is a close structural analogue of the collapsed tetragonal non-magnetic phase of CaFe_2As_2 . We find the Fermi surface of CaFe_2P_2 to differ from other related ternary phosphides in that its topology is highly dispersive in the c -axis, being three-dimensional in character and with identical mass enhancement on both electron and hole pockets (~ 1.5). The dramatic change in topology of the Fermi surface suggests that in a state with reduced (c/a) ratio, when bonding between pnictogen layers becomes important, the Fermi surface sheets are unlikely to be nested.

The nature of the Fermi surface dimensionality and its proximity to nesting in the iron-pnictide superconductors is at the core of understanding the mechanism of superconductivity. An important finding is that under *hydrostatic* pressure, BaFe_2As_2 and SrFe_2As_2 [1] superconduct whereas CaFe_2As_2 does not [2]. Instead it undergoes a structural transition to a phase with a much reduced c -axis length which is known as the ‘collapsed tetragonal’ (cT) state. If pressure is applied using a non-hydrostatic medium CaFe_2As_2 does become superconducting [1, 3]. This suggests that small uniaxial pressure components stabilize the superconductivity in CaFe_2As_2 . Understanding why this happens in these materials and whether the Fermi surface nesting or the strong coupling with the lattice are the relevant parameters will be important for understanding the origin of superconductivity in iron pnictides.

CaFe_2As_2 has three distinct magnetic and structural phases. Like many other iron-arsenides, at zero pressure, the high temperature tetragonal state becomes orthorhombic and antiferromagnetically ordered below $T_N \simeq 170$ K. At low temperatures under a pressure of 0.35 GPa there is a transition to the cT state in which there is a $\sim 10\%$ decrease in the c -axis lattice parameter and a $\sim 2\%$ increase in the a -axis [4]. Recent bandstructure calculations [5, 6] suggest that these phase transitions have a dramatic effect on the Fermi surface. In the high temperature tetragonal phase the Fermi surface is predicted to be similar to the other 122 pnictide consisting of two strongly warped electron cylinders at the Brillouin zone corners and hole cylinders at the center of the zone (Γ). Calculations suggest that these hole pockets are sensitive to structural details of the As position and the c -lattice constant, whereas the electron pockets are less affected [5]. However, in the cT state the calculated Fermi surface suffers a major topological change; the two electron cylinders at the zone corners transform into a single warped cylinder whereas the hole cylinders become a large three dimensional sheet.

The Fermi surface of many iron-pnictides have been extensively studied by angle resolved photoemission spectroscopy,

however so-far the cT phase of CaFe_2As_2 has been inaccessible to this technique because of the high pressures involved. Quantum oscillation (QO) studies have the advantage of probing precisely the bulk three dimensional Fermi surface but so far have only been possible in the magnetically ordered phase of the iron-arsenides [7] as the tetragonal superconducting phase cannot be accessed because of the high values of the upper critical field (~ 100 T). Although QO studies are possible under high pressure, these measurements are technically very challenging. One route to provide an insight into the Fermi surface properties of the iron-arsenides is to study the analogous non-magnetic phosphide materials. These materials have almost identical calculated Fermi surfaces to the arsenides in their non-magnetic state but are either non-superconducting or have a low T_c (and low H_{c2}) and single crystals can be grown with very high purity making them ideal for QO studies. Quantum oscillations have been measured in superconducting LaFePO [8] (which is analogous to the non-magnetic ‘1111’ arsenides e.g., LaFeAsO) and SrFe_2P_2 [9] (which is a structural analogue to the non-magnetic tetragonal ‘122’ arsenides).

Here we report a de Haas-van Alphen effect study of the Fermi surface of CaFe_2P_2 which is a very close structural analogue of the cT phase of CaFe_2As_2 . The isoelectric substitution of As with P does not change the number of Fe 3d electrons, but enhances P-P hybridization causing the lattice to contract in the c direction. Consequently the interlayer P-P distance approaches the molecular bond length [10], just as the As-As distance does in the cT phase [11]. We show experimentally that the Fermi surface of CaFe_2P_2 is different from the multiband electron-hole structure found in SrFe_2P_2 [9] and other pnictides, and is formed of a single warped cylinder and a large three dimensional hole sheet. We find a isotropic mass enhancements on the electron and hole sheets (~ 1.5).

High quality single crystals of CaFe_2P_2 were grown from a Sn flux similar to previous reports [9]. The residual resistivity ratio $\rho(300\text{K})/\rho(1.8\text{K})$ was measured to be greater than 120.

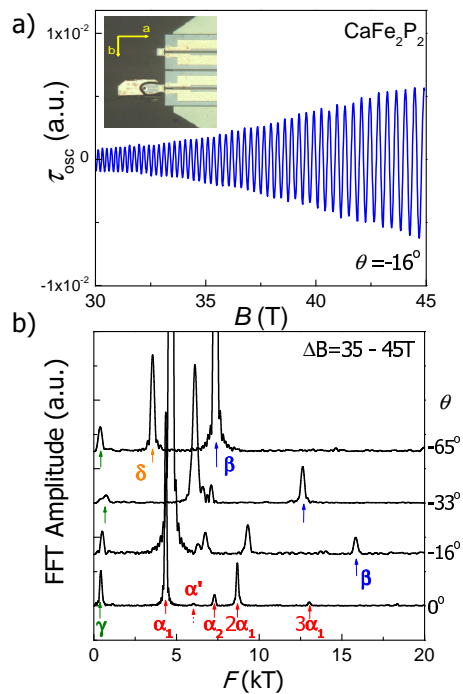


FIG. 1: (color online) a) Oscillatory part of torque at $T = 0.4$ K for a single crystal of CaFe_2P_2 (sample A). The inset shows sample A attached to a piezocantilever. b) The Fourier transform spectra showing the evolution of the extremal areas of the Fermi surface with the field angle, θ . The positions of different pockets, α_1 , α_2 , β , γ , δ and harmonics ($2\alpha_1$, $3\alpha_1$) as well as a weak peak, α' are indicated by arrows.

Torque magnetometry was performed using piezoresistive microcantilevers in high fields 18 T in Bristol (sample B) and 45 T (sample A) at the NHFML, Tallahassee. We compare our data with the predictions of bandstructure calculations which we performed using an augmented plane wave plus local orbital method as implemented in the WIEN2K code [12]. The experimentally determined lattice parameters and internal positions were used for these calculations [13].

Fig. 1(a) shows the oscillatory part of raw torque signal for a CaFe_2P_2 crystal up to 45 T. The fast Fourier transform (FFT) for several other orientations as the field is rotated from $B||c$ ($\theta = 0$) towards $B||a$ ($\theta = 90^\circ$) is shown in Fig.1b. The FFT frequencies F of oscillatory torque data (in the $1/B$ domain) are related to extremal Fermi surface areas by $F = (\hbar/2\pi e)A_k$. Close to $B||c$ the strongest amplitude peak (α_1) is at 4.35 kT and we also observe several harmonics of α_1 (see Fig.1b); we can distinguish a frequency $\alpha_2 \sim 7.3$ kT and a tiny feature α' at 6 kT [14]. A small pocket γ is observed at ~ 420 T; at higher angles ($\theta = 15^\circ$) the amplitude of another frequency, β , becomes significant and the position of this peak varies strongly with increasing angle. When we rotate close to $B||a$ a strong amplitude signal, δ , corresponding to an extremal area of 3.2 kT is found.

The angular dependence of the observed dHvA frequencies

allows us to identify the shape of the Fermi surface sheets from which they originate (see Fig. 2). Rotating away from $B||c$ the α_1 and α_2 orbits display a much stronger angular variation compared to extremal orbits on a simple cylinder with a weak k_z dispersion ($F(\theta) \sim 1/\cos\theta$), [8]. This suggests that these orbits originate from a strongly warped cylindrical Fermi surface [14]. The size of the β orbit changes dramatically with θ suggesting that this Fermi surface sheet has an prolate ellipsoidal shape with a maximum at $\theta = 0^\circ$. The α orbits are well reproduced in both samples, but the β orbit was only observed in sample A in much higher fields (up to 45 T). This can be explained as the impurity damping of the dHvA signal is proportional to $\exp(-k_F/(\ell B))$ so that higher field are needed to see the larger β orbit ($k_F \propto \sqrt{F}$) for the same mean-free-path (ℓ).

We now compared the experimental data in CaFe_2P_2 to the predictions of the band structure calculations. The Fermi surface (see Fig. 2 and Fig. 3) is quasi-three dimensional and is composed of a large hole sheet in the form of a flat pillow at the top of the zone whereas the electron sheets are strongly distorted quasi-two-dimensional tubes centered on the zone corners. There are also two tiny hole pockets centered at Z (see the bottom panel of Fig.3) containing only ~ 0.008 holes compared with the large hole and electron sheets which each contains ~ 0.41 holes/electrons; if the P position is optimized in the calculation (by minimising the total energy, $z_P=0.3890$) they disappear.

Fig. 2 shows good agreement between data and calculation in the case of the β frequency which corresponds to cross sections on the hole sheet (band 3) and the α_1 and α_2 frequencies which correspond to the minimum and maximal extremal areas of the strongly warped electron cylinder (band 4) (the degree of warping is roughly $\Delta F/F \sim 50\%$ in CaFe_2P_2 as compared with $\sim 23\%$ in SrFe_2P_2 [9]). The complex in-plane and interplane corrugations of the Fermi surface could give rise to additional branches not predicted by our calculations. This could explain the origin of the δ branch, which is observed within $\sim 25^\circ$ of $\theta = 90^\circ$ ($B||a$) (Fig. 2) and may account for the small shift found for α_2 as well as the presence of the weak feature at α' . It is worth emphasizing that the agreement between data and calculations (± 10 meV) for the main sheets is good in contrast to our findings for LaFePO and SrFe_2P_2 [8, 9] where rigid band shift of up to 100 meV were needed to bring the bandstructure into agreement with experiment.

Any small band shifts would mainly affect the small pockets of the Fermi surface centered at the Z point, as stated earlier. For example, by shifting the hole bands down the tiny pockets at the Z point disappear and the large hole pillow transforms into a large torroid [15]; when $B||a$ we could expect orbits from extremal areas on such torroid which may give rise to the δ branch (which is about half the size of the β orbit close to $B||a$) (see bottom panel of Fig. 3). The γ frequency increases to about $\theta = 42(3)^\circ$ and then decrease suggesting that it has a short closed cylinder shape (see Fig. 2). By shifting the hole bands up (by ~ 40 meV) the small 3D

TABLE I: Experimental and calculated Fermi surface parameters of CaFe_2P_2 close to $\theta = 0^\circ$ ($B_{\parallel c}$) similar to those predicted for CaFe_2As_2 in the cT phase [6].

	Experiment			Calculations			
	$F(\text{kT})$	$\frac{m^*}{m_e}$	$\ell(\text{nm})$	Orbit	$F(\text{kT})$	$\frac{m_b}{m_e}$	$\frac{m^*}{m_b}$
$\alpha_1(e)$	4.347	2.05(4)	190	4_{min}	4.439	1.38	1.49(3)
$\alpha_2(e)$	7.295	3.48(7)	71	4_{max}	7.837	2.40	1.45(3)
$\beta(h)$	18.360	4.0(2)	86	3_{min}	18.407	2.65	1.51(8)

pocket centered at the Z point (band 2) could be assigned to the γ branch (Fig.3). Alternatively, γ which has a low effective mass ($m^* = 0.4m_e$) could originate from an Sn impurity phase which has orbits with similar frequencies and masses [16], but x-ray diffraction measurements does not identify any Sn impurities at the level of $\sim 1\%$. In any case this pocket, γ , accounts for only a tiny fraction of holes (~ 0.03) and we believe it is unlikely to play any major role.

Fig. 3 shows a comparison between the Fermi surface of CaFe_2As_2 in the tetragonal phase ($c/a=2.98$), CaFe_2As_2 in the cT phase ($c/a=2.66$ at $P=0.63$ GPa) and CaFe_2P_2 ($c/a=2.59$). As mentioned before, it is clear that there is a remarkable similarity between CaFe_2P_2 and the cT phase of CaFe_2As_2 . Thus in CaFe_2As_2 applying *chemical pressure* (by the isoelectronic substitution of As by P) is equivalent to *applied hydrostatic pressure*, as found in other ternary pnictides [17]. This state of reduced c/a ratio has a different Fermi surface topology compared to CaFe_2As_2 or SrFe_2P_2 ($c/a=3.03$). Yildirim [11] has argued that the cT phase of CaFe_2As_2 occurs when, by reducing the Fe moment, the Fe-As bonding weakens and the (inter and intra-planar) As-As bonding gets stronger causing the significant strong reduction in the c axis [4]. Similarly, in non-magnetic phosphides, the reduction in the c -axis (or the c/a ratio) results in an increase P-P hybridization between pnictogen ions along the c direction (close to the single bond distance) [10]. The spacer between the iron layers (Sr or Ba) limits the degree of this hybridization between layers and such a state with *strong pnictogen bonding* is unlikely to occur [5, 17].

The effective masses, m^* , of CaFe_2P_2 for each Fermi surface orbit extracted from the temperature dependence of the dHvA signals, using the conventional Lifshitz-Kosevich formula [18], are shown in Table I and compared to the corresponding bandstructure values. The masses for the electron and hole sheets are enhanced by the same factor of ~ 1.5 in contrast to the sheet dependent variation of the enhancement observed recently in SrFe_2P_2 (which has two electron and two hole Fermi surface pockets). By comparing the quasiparticle enhancement on the electron sheets (which have the largest mean free path and often match better to the bandstructure calculations being less sensitive to structural changes compared with the hole pockets) we observe that in LaFePO the average enhancement is 2.38 (2.2 for inner and 2.54 for outer pocket) [8] whereas in SrFe_2P_2 is 1.85 (1.6 for inner and 2.1 for the outer electron sheet)[9]. The conventional electron-

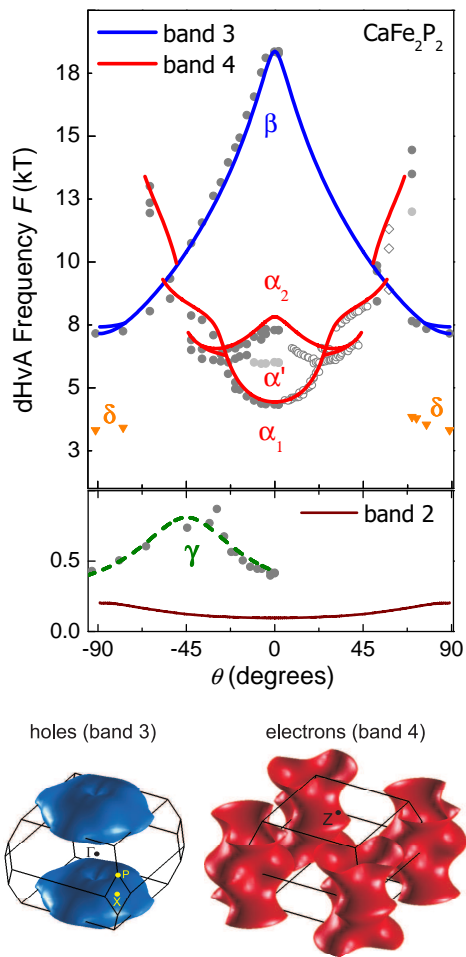


FIG. 2: (color online) Angle dependence of all observed frequencies compared with the band structure predictions (solid lines). Different symbols correspond to sample A (filled circles) and sample B (open circles). Solid grey points indicate the position of very weak features. The bottom panel shows an expanded low frequency scale for the γ pocket and the dotted line is a guide to the eye. The calculated Fermi surface of CaFe_2P_2 is also shown. The solid lines delimit the Brillouin zone and the Fermi surface sheets are represented in an extended zone.

phonon coupling, λ_{e-ph} , in the cT phase of CaFe_2As_2 is calculated to be 0.23 [11] but such calculations for CaFe_2P_2 are not yet available. Due to their structural and electronic similarities it is likely that in CaFe_2P_2 a mass enhancement of 1.23 could be due to a conventional electron-phonon coupling, but other effects could also be important [19]. The further anisotropic mass enhancement observed in LaFePO and possibly in SrFe_2P_2 could have another origin and may be related to the nesting of the Fermi surface. The mean free paths, ℓ , of the minimum electronic orbit is a factor 2 larger than that of large hole sheet and of the maximum electronic orbit. This suggests both anisotropy in scattering between electron and holes but also along k_z , as also observed in SrFe_2P_2 and LaFePO [8, 9].

In the case of the superconducting LaFePO and SrFe_2P_2

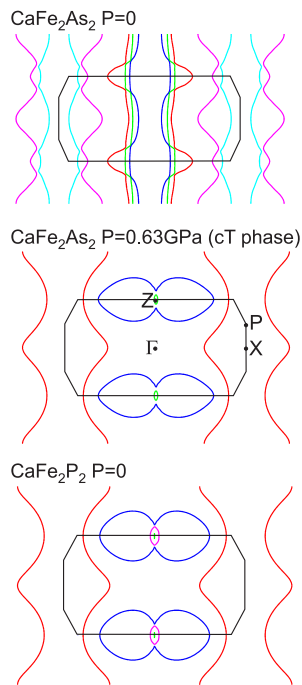


FIG. 3: (color online) Comparison of the calculated Fermi surface topology of CaFe_2As_2 (tetragonal phase), CaFe_2As_2 (cT phase) and CaFe_2P_2 . Slices through the center of the Brillouin zone (solid lines) in the (110) plane are shown.

[8, 9] the energies in the band structure were shifted in opposite direction for the electron and hole pockets to match up the experimental data. These asymmetric band shifts are suggested to result from geometric nesting [22]. In the present measurements on CaFe_2P_2 no band shifts were required ($\sim \pm 10$ meV) to achieve agreement with experiment and considering this model it would imply the absence of nesting in CaFe_2P_2 (or the lack of long-range order in the cT phase of CaFe_2As_2 [21].)

In conclusion, we have experimentally determined the Fermi surface of CaFe_2P_2 which is closely related to the collapsed tetragonal phase of CaFe_2As_2 . We find that the Fermi surface is composed of a single highly dispersive electron cylinder at the zone corners and a large three dimensional pillow shaped hole surface. The mass enhancement due to many-body interactions is isotropic (~ 1.5) and may be dominated by the electron-phonon coupling. The features of this Fermi surface which does not fulfill nesting condition is likely to be shared by the non-magnetic cT phase of CaFe_2As_2 and other ternary pnictides with reduced c/a ratio and may explain why

superconductivity is absent in such a state.

We thank M. Haddow and E. Yelland for technical support. We acknowledge financial support from the Royal Society, EPSRC, and EU 6th Framework contract RII3-CT-2004-506239. Work at Stanford was supported by the U.S. DOE, Office of Basic Energy Sciences under contract DE-AC02-76SF00515. Work performed at the NHMFL in Tallahassee, Florida, was supported by NSF Cooperative Agreement No. DMR-0654118, by the State of Florida, and by the DOE.

-
- [1] P. Alireza, *et al.*, J. Phys. Cond. Mat. **21**, 012208 (2008).
 - [2] W. Yu, *et al.*, Phys. Rev. B **79**, 020511 (2009).
 - [3] M. S. Torikachvili, S. L. Bud'ko, N. Ni, and P. C. Canfield, Phys. Rev. Lett. **101**, 057006 (2008).
 - [4] A. Kreyssig, *et al.*, Phys. Rev. B **78**, 184517 (2008).
 - [5] Y.-Z. Zhang, H. C. Kandpal, I. Opahle, H. O. Jeschke, and R. Valentí, arXiv:0812.2920 (2008).
 - [6] D. A. Tompsett and G. G. Lonzarich, arXiv:0902.4859.
 - [7] J. G. Analytis, *et al.*, arXiv:0902.1172.
 - [8] A. I. Coldea, *et al.*, Phys. Rev. Lett. **101**, 216402 (2008).
 - [9] J. G. Analytis, *et al.*, arXiv:0904.2405.
 - [10] E. Gustenau, P. Herzig, and A. Neckel, J. Solid State Chem. **129**, 147 (1997).
 - [11] T. Yildirim, Phys. Rev. Lett. **102**, 037003 (2009).
 - [12] P. Blaha, K. Schwarz, G. K. H. Madsen, D. Kvasnicka, and J. Luitz, *WIEN2K, An Augmented Plane Wave + Local Orbitals Program for Calculating Crystal Properties* (Karlheinz Schwarz, Techn. Universität Wien, Austria, 2001).
 - [13] $a=3.855$ Å, $c=9.985$ Å, and $z_P=0.3643$ for CaFe_2P_2 [24], $a=3.8915$ Å, $c=11.690$ Å, and $z_P=0.372$ for CaFe_2As_2 [4], and $a=3.978$ Å, $c=10.607$ Å, and $z_P=0.3663$ for CaFe_2As_2 in the cT phase ($p=0.63$ GPa) [4].
 - [14] The X-ray diffraction shows that sample A contain a single domain with a ($\sim 1^\circ$) mosaic spread and about one percent of another phase missaligned in the (ac) plane.
 - [15] P. M. C. Rourke, *et al.*, Phys. Rev. Lett. **101**, 237205 (2008).
 - [16] J. E. Craven, Phys. Rev. B **182**, 693 (1969).
 - [17] A. Kimber, S. A. J. and Kreyssig, *et al.*, Nature Materials (2009).
 - [18] D. Schoenberg, *Magnetic Oscillations in Metals* (Cambridge University Press, London, 1984).
 - [19] Many-body interactions could be responsible for a further enhancement of the electron-phonon interaction due the strong polarization of p-orbitals [20].
 - [20] M. Kulić and A. Haghighirad, arXiv:0904.3512.
 - [21] A. I. Goldman, *et al.*, Phys. Rev. B **79**, 024513 (2009).
 - [22] L. Ortenzi, E. Cappelluti, L. Benfatto, and L. Pietronero, arXiv:0903.0315.
 - [23] T. Kondo, *et al.*, arXiv:0905.0271.
 - [24] A. Mewis, Z. Naturforsch. B **35B**, 391 (2009).